ChemComm

COMMUNICATION

View Article Online
View Journal | View Issue



Cite this: *Chem. Commun.*, 2015, **51**, 15145

Received 19th June 2015,
Accepted 21st August 2015

DOI: 10.1039/c5cc05064b

www.rsc.org/chemcomm

# Mechanism of a one-photon two-electron process in photocatalytic hydrogen evolution from ascorbic acid with a cobalt chlorin complex†

Shoko Aoi,[a] Kentaro Mase,[a] Kei Ohkubo[ab] and Shunichi Fukuzumi*[abc]

**A one-photon two-electron process was made possible in photocatalytic $H_2$ evolution from ascorbic acid with a cobalt(II) chlorin complex [$Co^{II}$(Ch)] *via* electron transfer from ascorbate to the excited state of $[Ru(bpy)_3]^{2+}$ followed by electron transfer from $[Ru(bpy)_3]^{+}$ to $Co^{II}$(Ch) with proton to give the hydride complex, which reacts with proton to produce $H_2$. [$Co^{III}$(Ch)]$^+$ was reduced by ascorbate to reproduce $Co^{II}$(Ch).**

Photocatalytic production of hydrogen ($H_2$) has attracted increasing attention as a clean energy source because of the ever-increasing demand for energy and climate change on our planet.[1] A number of highly efficient hydrogen evolving systems have been developed including homogeneous and heterogeneous photocatalytic systems.[2–13] Two electrons are required to produce $H_2$ from protons, although one photon generates normally only one electron. A mechanism of photocatalytic production of $H_2$ was reported to clarify how photoinduced electron transfer of a photosensitiser (a one-electron process) leads to $H_2$ production (a two-electron process).[14–16] Disproportionation of one-electron reduced species of metal complexes resulted in formation of the two-electron reduced species from which $H_2$ is formed.[17] Bimolecular reactions of metal(III)–hydride complexes also generate $H_2$ accompanied by regeneration of metal(II) complexes.[18] In each case, the maximum quantum yield of $H_2$ production per photon is 50%, because two photons are required to produce two electrons. Thus there has so far been no example for one photon to generate one $H_2$ molecule.

We report herein photocatalytic $H_2$ evolution from ascorbic acid ($AscH_2$) with a cobalt(II) chlorin complex [$Co^{II}$(Ch)] (a chemical structure shown in Scheme 1)[19] in an aqueous acetonitrile solution ($H_2O$/MeCN), which proceeds *via* a one-photon two-electron process. The photocatalytic mechanism is clarified by nanosecond laser transient absorption spectra and by examining each step in the catalytic cycle independently.

Visible light irradiation of a deaerated (Ar-saturated) $H_2O$/MeCN solution (1 : 1 v/v) of $[Ru(bpy)_3]^{2+}$ (bpy = 2,2′-bipyridine) containing ascorbic acid ($AscH_2$) and ascorbate ($AscH^-$) ($E_{ox}$ = 0.43 V *vs.* SCE) as an electron donor and $Co^{II}$(Ch) ($E_{red}$ = −0.96 V *vs.* SCE) (Fig. S1 in the ESI†) as a catalyst resulted in $H_2$ evolution (Fig. 1, black line). When the ratio of $AscH^-$ to $AscH_2$ was changed as fixed total concentrations of $AscH_2$ and $AscH^-$ ([$AscH_2$] + [$AscH^-$] = 1.1 M), the largest $H_2$ evolution activity was attained with $AscH^-$ (0.30 M) and $AscH_2$ (0.80 M) (Fig. S2 in ESI†). The smaller concentration of $AscH^-$ results in less efficient reductive quenching of the $[Ru(bpy)_3]^{2+}$* emission (* denotes the excited state).

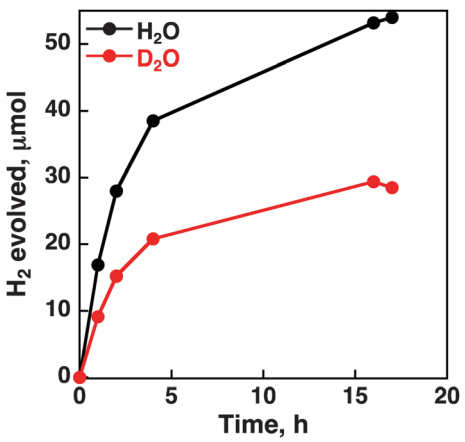


Fig. 1 Time courses of $H_2$ evolution in the photocatalytic reduction of proton in an Ar-saturated $H_2O$/MeCN (black) and $D_2O$/MeCN (red) mixed solution (1 : 1 v/v) containing $[Ru^{II}(bpy)_3]^{2+}$ (2.0 mM), $AscH_2$ (0.80 M), AscHNa (0.30 M) and $Co^{II}$(Ch) (25 μM) under irradiation of visible light ($\lambda$ > 420 nm) at 298 K.

[a] *Department of Material and Life Science, Graduate School of Engineering, Osaka University, ALCA and SENTAN, Japan Science and Technology Agency (JST), Suita, Osaka 565-0871, Japan. E-mail: fukuzumi@chem.eng.osaka-u.ac.jp; Fax: +81-6-6879-7370*

[b] *Department of Chemistry and Nano Science, Ewha Womans University, Seoul 120-750, Korea*

[c] *Faculty of Science and Technology, Meijo University, ALCA and SENTAN, Japan Science and Technology Agency (JST), Nagoya, Aichi 468-8502, Japan*

† Electronic supplementary information (ESI) available: Experimental details and cyclic voltammograms (Fig. S1), time courses of $H_2$ evolution (Fig. S2), emission spectra (Fig. S3 and S5), UV-vis absorption spectra (Fig. S4 and S7) and kinetic data (Fig. S6–S11). See DOI: 10.1039/c5cc05064b

The quenching efficiency of $[Ru(bpy)_3]^{2+*}$ ($E_{red}$ = 0.77 V *vs.* SCE in MeCN)[20] by $AscH^-$ (0.30 M) with $AscH_2$ (0.80 M) was determined to be 95% (Fig. S3 in ESI†). On the other hand, the smaller concentration of $AscH_2$ may retard $H_2$ production due to decreasing the acidity. When $H_2O$ was replaced by $D_2O$, $D_2$ and HD were produced without formation of $H_2$. Thus, hydrogen was produced from water and ascorbic acid as electron and proton sources. The observed deuterium kinetic isotope effect (KIE) in Fig. 1 ($k_H/k_D$ = 1.8 in the initial stage) suggests that the Co–H bond cleavage of a cobalt hydride intermediate ($[Co^{III}(H)(Ch)]$) by proton may be the rate-determining step for the photocatalytic $H_2$ evolution (*vide infra*).

The concentration of $Co^{II}(Ch)$ was optimised to be 50 μM for the efficient photocatalytic $H_2$ evolution. The absorption of $[Ru(bpy)_3]^{2+}$ is blocked by the larger concentration of $Co^{II}(Ch)$ (Fig. S4 in ESI†).[21] The quantum yield of the photocatalytic $H_2$ evolution was determined to be 12% using a ferric oxalate actinometer (see the Experimental section in ESI†). This value is similar to the highest value reported for photocatalytic $H_2$ evolution using a cobalt terpyridine complex ($\Phi$ = 0.13).[22]

Nanosecond transient absorption spectra of an $H_2O$/MeCN solution of $[Ru(bpy)_3]^{2+}$ with $AscH_2$ and $AscH^-$ are shown in Fig. 2, where appearance of the absorption band at 500 nm due to $[Ru(bpy)_3]^+$ is observed upon the nanosecond laser excitation. Thus, electron transfer from $AscH^-$ to $[Ru(bpy)_3]^{2+*}$ occurred to produce $AscH^\bullet$ and $[Ru(bpy)_3]^+$. The rate constant of electron transfer from $AscH^-$ to $[Ru(bpy)_3]^{2+*}$ ($k_{et}$) was determined to be $8.0 \times 10^8$ $M^{-1}$ $s^{-1}$ from a slope of Stern–Volmer plot ($K_{SV} = 3.5 \times 10^2$ $M^{-1}$) and the lifetime of $[Ru(bpy)_3]^{2+*}$ (0.44 μs in water/MeCN 1 : 1 v/v) (Fig. S5 in ESI†).[23] The decay rate of absorbance at 500 nm due to $[Ru(bpy)_3]^+$ obeyed the second-order kinetics of bimolecular back electron transfer from $[Ru(bpy)_3]^+$ to $AscH^\bullet$. In the presence of $Co^{II}(Ch)$, the decay of absorbance became much faster because of electron transfer from $[Ru(bpy)_3]^+$ to $Co^{II}(Ch)$ as shown in Fig. 2b. The decay rate constant linearly increased with increasing the concentration of $[Co^{II}(Ch)]$ (Fig. S6 in ESI†). The rate constant of electron transfer from $[Ru(bpy)_3]^+$ to $Co^{II}(Ch)$ was determined to be $2.5 \times 10^9$ $M^{-1}$ $s^{-1}$ from the slope of dependence of the first-order decay rate constant on concentration of $Co^{II}(Ch)$ (Fig. S6b in ESI†).

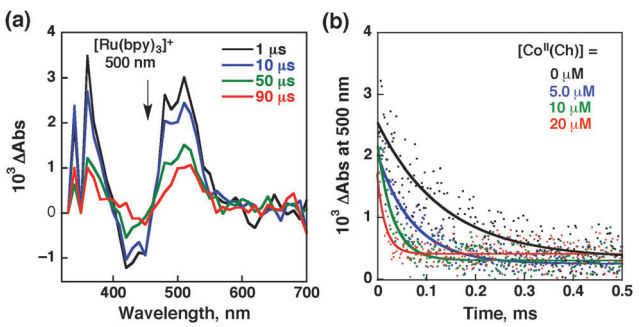


Fig. 2 (a) Transient absorption spectra after laser excitation ($\lambda$ = 450 nm) of $[Ru^{II}(bpy)_3]^{2+}$ (80 μM) in the presence of $AscH_2$ (0.80 M) and AscHNa (0.30 M) in a deaerated $H_2O$/MeCN mixed solution (1 : 1 v/v) at 298 K. (b) Time profiles of absorbance at 500 nm due to decay of $[Ru(bpy)_3]^+$ in the presence of various concentrations of $Co^{II}(Ch)$ (0–20 μM) in deaerated $H_2O$/MeCN mixed solutions (1 : 1 v/v) containing $[Ru^{II}(bpy)_3]^{2+}$ (80 μM), $AscH_2$ (0.80 M), AscHNa (0.30 M).

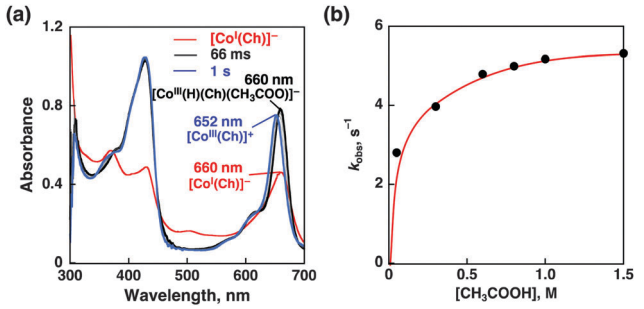


Fig. 3 (a) UV-vis absorption spectral changes of $[Co^I(Ch)]^-$ (30 μM) upon addition of $CH_3COOH$ (0.30 M) in deaerated MeCN at 298 K. The black and blue lines show the spectra taken at 66 ms and 1 s after mixing, respectively. The red line shows UV-vis absorption spectrum of $[Co^I(Ch)]^-$ (15 μM) formed by the electron-transfer reduction of $Co^{II}(Ch)$ (15 μM) with $CoCp_2^*$ (300 μM) in deaerated MeCN at 298 K. (b) Plot of $k_{obs}$ for the rate of formation of $[Co^{III}(Ch)]^+$ *vs.* $[CH_3COOH]$.

To examine the reaction of $[Co^I(Ch)]^-$ that is produced by electron transfer from $[Ru(bpy)_3]^+$ to $Co^{II}(Ch)$, $[Co^I(Ch)]^-$ was prepared by the one-electron reduction of $Co^{II}(Ch)$ by decamethylcobaltocene $[Co(Cp^*)_2]$ in MeCN (Fig. S7 in ESI†). The UV-vis absorption band of $[Co^I(Ch)]^-$ (red line in Fig. 3a; $\lambda_{max}$ = 510 nm) decreased with increasing absorption band at 660 nm (black line) at 66 ms after addition of acetic acid ($CH_3COOH$) (0.30 M). Then, this absorption band was finally blue shifted to $\lambda_{max}$ = 652 nm, which is due to $[Co^{III}(Ch)]^+$.[24,25] Thus, $[Co^I(Ch)]^-$ may react with $CH_3COOH$ to form the hydride complex ($[Co^{III}(H)(Ch)(CH_3COO)]^-$: $\lambda_{max}$ = 660 nm), from which $H_2$ was evolved by the reaction with $CH_3COOH$ to produce $[Co^{III}(Ch)]^+$. The reaction of $[Co^I(Ch)]^-$ with $CH_3COOH$ was monitored by the absorption change at 652 nm due to $[Co^{III}(Ch)]^+$ as shown in Fig. 3, where the rate of the formation of $[Co^{III}(Ch)]^+$ obeyed first-order kinetics (Fig. S8 in ESI†). The first-order rate constant increased with increasing concentration of $CH_3COOH$ to approach a constant value (Fig. 3b). Such a saturation behaviour indicates that $CH_3COOH$ is not involved in the rate-determining step and that the reaction of $[Co^I(Ch)]^-$ with $CH_3COOH$ proceeds *via* formation of the hydride complex ($[Co^{III}(H)(Ch)(CH_3COO)]^-$), followed by the rate-determining heterolytic cleavage of the $Co^{III}$–H bond. The subsequent reaction of the released hydride ion with $CH_3COOH$ to produce $H_2$ and $[Co^{III}(Ch)]^+$ may be fast as compared with the back reaction of the $Co^{III}$–H bond cleavage (Scheme 1). The kinetic equation for the formation of $[Co^{III}(Ch)]^+$ is given by eqn (1),

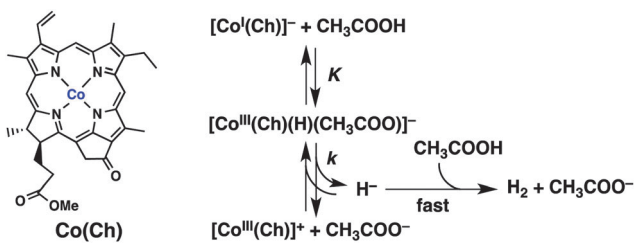


Scheme 1 Mechanism of hydrogen formation by the reaction of $[Co^I(Ch)]^-$ with $CH_3COOH$.

$$d[[Co^{III}(Ch)]^+]/dt = k[[Co^{III}(H)(Ch)(CH_3COO)]^-] \quad (1)$$

where $k$ is the rate constant of the hydrogen evolution. From the equilibrium constant ($K$), the concentration of a complex between $[Co^{I}(Ch)]^-$ and $CH_3COOH$ is given by eqn (2), where

$$[[Co^{III}(H)(Ch)(CH_3COO)]^-] = K[CH_3COOH]([[Co^{I}(Ch)]^-]_0 - [[Co^{III}(Ch)]^+])/(1 + K[CH_3COOH]) \quad (2)$$

$[[Co^{I}(Ch)]^-]_0$ is the initial concentration. Eqn (1) is rewritten by eqn (3).

$$d[[Co^{III}(Ch)]^+]/dt = kK[CH_3COOH]([[Co^{I}(Ch)]^-]_0 - [[Co^{III}(Ch)]^+])/(1 + K[CH_3COOH]) \quad (3)$$

Under the conditions, the concentration of $CH_3COOH$ is much higher than that of $[Co^{I}(Ch)]^-$, the $k_{obs}$ value is given by eqn (4). To determine the $k$ value, eqn (4) is rewritten by eqn (5), which predicts

$$k_{obs} = kK[CH_3COOH]/(1 + K[CH_3COOH]) \quad (4)$$

$$k_{obs}^{-1} = 1/kK\cdot[CH_3COOH]^{-1} + 1/k \quad (5)$$

a linear correlation between $k_{obs}^{-1}$ and $[CH_3COOH]^{-1}$ (Fig. S9 in ESI†). The $k$ and $K$ values were determined from the intercept and slope of the linear plot of $k_{obs}^{-1}$ *vs.* $[CH_3COOH]^{-1}$ to be 5.9 $s^{-1}$ and 7.1 $M^{-1}$.

When $CH_3COOH$ was replaced by $CH_3COOD$, the deuterium kinetic isotope effect (KIE) was observed (Fig. S10 in ESI†),[26] indicating that the cleavage of the Co–H bond of $[Co^{III}(H)(Ch)(CH_3COO)]^-$ or O–H bond of $CH_3COOH$ is involved in the rate-determining step of the reaction of $[Co^{I}(Ch)]^-$ with $CH_3COOH$. Because $CH_3COOH$ is not involved in the rate-determining step (*vide infra*), the cleavage of the Co–H bond of $[Co^{III}(H)(Ch)(CH_3COO)]^-$ is the rate-determining step of the reaction of $[Co^{I}(Ch)]^-$ with $CH_3COOH$. The KIE value was 1.7 which is virtually the same as observed for the photocatalytic $H_2$ evolution (KIE = 1.8, Fig. 1), indicating that the heterolytic Co–H bond cleavage of $[Co^{III}(H)(Ch)(CH_3COO)]^-$ is also the rate-determining step in the photocatalytic $H_2$ evolution.

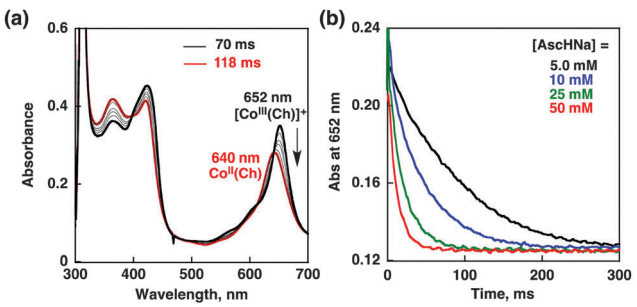


Fig. 4 (a) UV-vis absorption spectral changes in the electron-transfer reduction of $[Co^{III}(Ch)]^+$ (15 μM) with AscHNa (50 mM) in air-saturated $H_2O$/MeCN mixed solutions (1 : 1 v/v) at 298 K taken at 70 ms and 118 ms after mixing. (b) Decay time profiles of absorbance at 652 nm due to $[Co^{III}(Ch)]^+$ in the presence of various concentrations of AscHNa in air-saturated $H_2O$/MeCN mixed solutions (1 : 1 v/v) at 298 K.

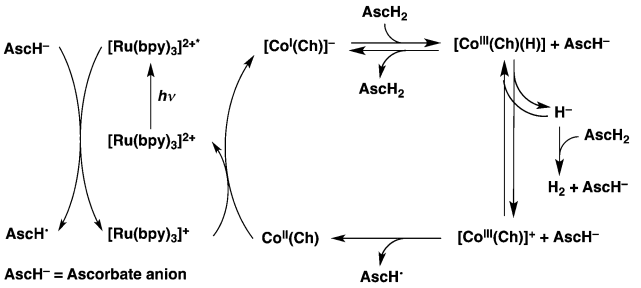


Scheme 2 Mechanism of photocatalytic hydrogen evolution from $AscH^-$ and $AscH_2$ with $[Ru(bpy)_3]^{2+}$ and $Co^{II}(Ch)$.

$[Co^{III}(Ch)]^+$ produced by the reaction of $[Co^{III}(H)(Ch)(CH_3COO)]^-$ with $CH_3COOH$ is reduced by $AscH^-$ to form $Co^{II}(Ch)$ as shown by stopped-flow measurements in Fig. 4.[27] The rate constant of electron transfer from $AscH^-$ to $[Co^{III}(Ch)]^+$ that was prepared by the one-electron oxidation of $Co^{II}(Ch)$ with $(p\text{-}BrC_6H_4)_3N^{\bullet+}SbCl_6^-$ in $H_2O$/MeCN was determined to be $1.5 \times 10^3$ $M^{-1}$ $s^{-1}$ from the linear dependence of the first-order rate constant on concentration of $AscH^-$ (Fig. S11 in ESI†).

The photocatalytic cycle is summarized in Scheme 2. Photoexcitation of $[Ru(bpy)_3]^{2+}$ resulted in electron transfer from $AscH^-$ to $[Ru(bpy)_3]^{2+*}$ to produce $[Ru(bpy)_3]^+$, followed by electron transfer from $[Ru(bpy)_3]^+$ to $Co^{II}(Ch)$ to produce $[Co^{I}(Ch)]^-$, which reacts with $AscH_2$ to produce $[Co^{III}(H)(Ch)(AscH)]^-$. Hydrogen is generated by the reaction of $[Co^{III}(H)(Ch)(AscH)]^-$ with $AscH_2$ *via* the Co–H bond heterolysis to produce $[Co^{III}(Ch)]^+$,[28,29] which is reduced by $AscH^-$ to regenerate $Co^{II}(Ch)$. In such a case, a one-photon two-electron process is made possible, because one photon is required to produce $[Co^{I}(Ch)]^-$ for $H_2$ evolution and another electron is provided thermally by $AscH^-$.

In conclusion, $Co^{II}(Ch)$ acts as an efficient catalyst for photocatalytic $H_2$ evolution from ascorbic acid with $[Ru(bpy)_3]^{2+}$ as a photocatalyst to attain the high quantum yield *via* a one-photon two-electron process in which the second electron is provided thermally from ascorbic acid.

This work was supported by Grants-in-Aid (no. 26620154 and 26288037 to K.O.) and JSPS fellowship (No. 25-727 to K.M.) from the Ministry of Education, Culture, Sports, Science and Technology (MEXT); ALCA and SENTAN projects from JST, Japan (to S.F.).

## Notes and references

1 R. A. Kerr and R. F. Service, *Science*, 2005, **309**, 101.
2 X. Song, H. Wen, C. Ma, H. Chen and C. Chen, *New J. Chem.*, 2015, **39**, 1734.
3 K. Kawano, K. Yamauchi and K. Sakai, *Chem. Commun.*, 2014, **50**, 9872.
4 X. Wang, S. Goeb, Z. Ji, N. A. Pogulaichenko and F. N. Castellano, *Inorg. Chem.*, 2011, **50**, 705.
5 L.-Z. Fu, L.-L. Zhou, L.-Z. Tang, Y.-X. Xhang and S.-Z. Zhan, *J. Power Sources*, 2015, **280**, 453.
6 S. Fukuzumi, *Curr. Opin. Chem. Biol.*, 2015, **25**, 18.
7 D. Basu, S. Mazumder, X. Shi, H. Baydoun, J. Niklas, O. Poluektov, H. B. Schlegel and C. N. Verani, *Angew. Chem., Int. Ed.*, 2015, **54**, 2105.
8 A. Call, Z. Codola, F. Acuna-Pares and J. Lloret-Fillol, *Chem. – Eur. J.*, 2014, **20**, 6171.
9 H. Lv, W. Guo, K. Wu, Z. Chen, J. Bacsa, D. G. Musaev, Y. V. Geletii, S. M. Lauinger, T. Lian and C. L. Hill, *J. Am. Chem. Soc.*, 2014, **136**, 14015.

10 L. Chen, G. Chen, C.-F. Leung, S.-M. Yiu, C.-C. Ko, E. Anxolabéhère-Mallart, M. Robert and T.-C. Lau, *ACS Catal.*, 2015, **5**, 356.
11 A. Zarkadoulas, E. Koutsouri, C. Kefalidi and C. A. Mitsopoulou, *Coord. Chem. Rev.*, 2014, **11**, 6.
12 K. Maeda, M. Eguchi and T. Oshima, *Angew. Chem., Int. Ed.*, 2014, **53**, 13164.
13 J. Zhao, Y. Ding, J. Wei, X. Du, Y. Yu and R. Han, *Int. J. Hydrogen Energy*, 2014, **39**, 18908.
14 E. Deponti, A. Luisa, M. Natali, E. lengo and F. Scandola, *Dalton Trans.*, 2014, **43**, 16345.
15 H. Ozawa and K. Sakai, *Chem. Commun.*, 2011, **47**, 2227.
16 A. Rodenberg, M. Orazietti, B. Probst, C. Bachmann, R. Alberto, K. K. Baldridge and P. Hamm, *Inorg. Chem.*, 2015, **54**, 646.
17 S. Fukuzumi, T. Kobayashi and T. Suenobu, *Angew. Chem., Int. Ed.*, 2011, **50**, 728.
18 J. L. Dempsey, B. S. Brunschwig, J. R. Winkler and H. B. Gray, *Acc. Chem. Res.*, 2009, **42**, 1995.
19 K. Mase, K. Ohkubo and S. Fukuzumi, *J. Am. Chem. Soc.*, 2013, **135**, 2800.
20 J. Yuasa and S. Fukuzumi, *J. Am. Chem. Soc.*, 2006, **128**, 14281.
21 The photocatalytic $H_2$ evolution in our optimized conditions, the absorption at $\lambda$ = 450 nm of $[Ru(bpy)_3]^{2+}$ (2.0 mM, $\varepsilon_{450nm}$ = 1.4 × $10^4$ $M^{-1}$ $cm^{-1}$) is not significantly blocked by that of $Co^{II}$(Ch) ($Abs_{450nm}$ = 0.38; $\varepsilon_{450nm}$ = 1.8 × $10^4$ $M^{-1}$ $cm^{-1}$) under this experimental conditions.
22 C. V. Krishnan and N. Sutin, *J. Am. Chem. Soc.*, 1981, **103**, 2141.
23 The emission lifetime of $[Ru(bpy)_3]^{2+*}$ in water at 298 K was reported to be 0.58 μs; see: J. V. Houten and R. J. Watts, *J. Am. Chem. Soc.*, 1976, **98**, 4853.
24 The spectrum of $[Co^{III}(Ch)]^+$ obtained by the reaction $[Co^{I}(Ch)]^-$ with $CH_3COOH$ was identical to that of $[Co^{III}(Ch)]^+$ prepared by the electron-transfer oxidation of $Co^{II}$(Ch) by a one-electron oxidizing reagent of $(p\text{-}BrC_6H_4)_3N^{\bullet+}SbCl_6^-$ ($E_{red}$ = 1.05 V *vs.* SCE).[19].
25 $[Co^{III}(Ch)]^+$ or $Co^{III}$(H)(Ch) species is not re-reduced by large excess of $Co(Cp^*)_2$, under the present reaction conditions because $Co^{II}$(Ch) with 20 molar equiv. of $Co(Cp^*)_2$ is necessary to quantitatively produce $[Co^{I}(Ch)]^-$ as shown in ESI,† Fig. S7. $Co(Cp^*)_2$ ($E_{1/2}^{+/0}$ = −1.47 V *vs.* SCE) is unstable even in carefully degassed and dehydrated MeCN.
26 The KIE value was determined from the $k_{obs}$ values at $[CH_3COOH]$ = $[CH_3COOD]$ = 1.0 M.
27 Neither oxidation of $[Co^{III}(Ch)]^+$ nor $O_2$ reduction was observed under the basic reaction conditions.
28 S. Mandal, S. Shikano, Y. Yamada, Y.-M. Lee, W. Nam, A. Llobet and S. Fukuzumi, *J. Am. Chem. Soc.*, 2013, **135**, 15294.
29 No Co(II)–H complex is involved in the heterolysis of the Co–H bond as reported in ref. 28.

 